Journal of
Nanoscience and Nanotechnology
Vol. 11, 782–786, 2011

Structural and Optical Properties of Cu Doped ZnO Thin Films by Co-Sputtering

Sung Mook Chung*, Jae-Heon Shin, Jeong-Min Lee, Min Ki Ryu, Woo-Seok Cheong, Sang Hee Ko Park, Chi-Sun Hwang, and Kyoung Ik Cho

Convergence Components and Materials Research Laboratory, Electronics and Telecommunications Research Institute, 161 Gajeong-Dong, Yuseong-Gu, Daejeon 305-700, Korea

This paper reports on the structural and optical properties of ZnCuO thin films that were prepared by co-sputtering for the application of *p*-type-channel transparent thin-film transistors (TFTs). Pure ceramic ZnO and metal Cu targets were prepared for the co-sputtering of the ZnCuO thin films. The effects of the Cu concentration on the structural, optical, and electrical properties of the ZnCuO films were investigated after their heat treatment. It was observed from the XRD measurements that the ZnCuO films with a Cu concentration of 7% had ZnO(002), Cu_2O(111), and Cu_2O(200) planes. The 7% Cu-doped ZnO films also showed a band-gap energy of ~2.05 eV, an average transmittance of ~62%, and a *p*-type carrier density of $\sim 1.33 \times 10^{19}$ cm^{-3} at room temperature. The bottom-gated TFTs that were fabricated with the ZnCuO thin film as a *p*-type channel exhibited an on-off ratio of ~6. These results indicate the possibility of applying ZnCuO thin films with variable band-gap energies to ZnO-based optoelectronic devices.

Keywords: ZnCuO Thin Films, Co-Sputtering, *p*-Type, TFT.

RESEARCH ARTICLE

1. INTRODUCTION

Zinc oxide (ZnO) has been considered a promising material for high-temperature electronics, transparent high-power electronics, surface acoustic wave devices, optoelectronic devices, ultraviolet (UV) light-emitting diodes, varistors, and laser diodes.[1–5] ZnO is a wide direct band-gap (E_g: ~ 3.37 eV) semiconductor that has a large exciton binding energy of 60 meV at room temperature, with a low lasing threshold density.[3] To realize high-performance ZnO-based optoelectronic devices, however, one of the most important requirements is band-gap engineering.[4] The resistivity of ZnO films may be adjusted between 10^{-4} and 10^{12} Ωcm by doping and changing the annealing conditions.[6–7] To improve the conductivity of ZnO films, various impurity dopants have been attempted, such as Al, Ga, Ti, In, B, and H for *n*-type ZnO, and N and As for *p*-type ZnO.[4–9] Achieving a high-quality *p*-type ZnO has been a major challenge in the fabrication of long-lasting and robust electrooptic devices.[10] Various research groups have recently started working on the synthesis of several *p*-type transparent conducting oxide thin films and on the fabrication of devices that use them.[7–10] While the fabrication of *n*-type ZnO films is easy with a high carrier concentration even without any doping, the fabrication of *p*-type ZnO films is difficult due to the self-compensation effect that involves native defects such as oxygen vacancies (V_o) and zinc interstitials (Zn_i).[11] Copper (Cu) is a non-toxic, economical, and abundant resource, which makes copper oxide an interesting material.[12] ZnO:Cu films are usually fabricated for their electrical and ferromagnetic properties.[13] It has also been demonstrated that ZnO films doped with Cu have higher electrical resistance and *c*-axis-crystallite preference.[14, 15] Moreover, it is well known that a Cu atom, as a group Ib element, can also act as an acceptor in ZnO if it is incorporated into a substitional Zn site.[16, 17]

In this paper, the structural and optical properties of ZnCuO thin films that were prepared by co-sputtering for the application of *p*-type-channel transparent TFTs is reported. Pure ceramic ZnO and metal Cu targets were prepared for the co-sputtering of the ZnCuO thin films. The effects of the Cu concentration on the structural, optical, and electrical properties of the ZnCuO films were investigated after their heat treatment. Bottom-gated TFTs were also fabricated with the ZnCuO thin film as a *p*-type channel.

2. EXPERIMENTAL DETAILS

ZnCuO thin films were deposited on a Corning glass 1737 by radio frequency (rf) sputtering of ZnO and direct

*Author to whom correspondence should be addressed.

1533-4880/2011/11/782/005 doi:10.1166/jnn.2011.3157

current (dc) sputtering of Cu. Pure ceramic ZnO and metal Cu targets were synthesized for the co-sputtering of the ZnCuO thin films. The substrates were ultrasonically cleaned in acetone and methanol, and finally rinsed in deionized water. The base vacuum in the chamber was made to go down to 5×10^{-7} Torr. Argon gas with a little additional oxygen (<0.1%) was made to flow into the chamber for the sputtering. The substrate temperature and working pressure were 550 °C and 10 mTorr, respectively. The heat treatment of the films was carried out in a vacuum furnace for 1 h at 700 °C, with an oxygen flow of ~10 sccm. After the fabrication, the surface morphology and the film thickness were analyzed using a scanning electron microscope (SEM). The structural changes were observed using an X-ray diffractometer (XRD). The electrical parameters were estimated using the Hall measurement method in the van der Pauw configuration at room temperature. The transmittance measurement was performed using an ultraviolet-visible (UV-VIS) spectrophotometer.

To investigate the potential of the ZnCuO thin films for application in optoelectronic devices, the ZnCuO thin films were deposited on a thermal-oxide gate insulator and *n*-type Indium Zinc Oxide (IZO) thin films to form the *p*-type bottom-gate TFT and the hetero *p–n* junction structure, respectively. The thickness of the ZnCuO active layer for the TFTs was ~30 nm. The source and drain electrodes that consisted of an 8 nm-thick titanium (Ti) layer and a 100 nm-thick gold (Au) layer were deposited on the ZnCuO active layer via electron beam (E-beam) evaporation. The channel width (W) and length (L) of the ZnCuO TFTs were 100 μm and 1,000 μm, respectively. The electrical characteristics of the fabricated ZnCuO TFTs were measured using an Agilent 4156C semiconductor parameter analyzer at room temperature in a dark box.

3. RESULTS AND DISCUSSION

The XRD patterns of the ZnCuO films with various Cu concentrations are presented in Figure 1. The cuprite phase (Cu_2O) peaks were found only in the Cu(7%)-doped ZnO thin films. The diffraction peaks at $2\theta = 36.52$ and $2\theta = 36.25$ in the Cu(7%)-doped ZnO thin film might correspond to the $Cu_2O(111)$ and ZnO(101) phase peaks, respectively. All the ZnCuO films that were prouced by the argon gas with a little additional oxygen flow (<0.1%) exhibited a *c*-orientation peak (ZnO(002)). No secondary phase and metal-related peaks were detected in all the ZnCuO films within the sensitivity of XRD. The ZnO(002) peak position of all the ZnCuO films shifted by about 0.1°~0.2° towards the left, however, unlike that of the undoped ZnO. The peak shift illustrates the incorporation of a Cu ion into the ZnO lattice.[18,19] By calculating the lattice constant of the ZnCuO films, it was found that the cell parameters of a and c of the ZnCuO films had values of 0.3259 nm and 0.5242 nm, respectively, which are larger than those of the undoped ZnO film ($a = 0.3250$ nm and $c = 0.5207$ nm). Besides, the intensity of the (002) peak was observed to have been reduced with the incorporation of Cu in the films. Besides, the intensity of the (002) peak is observed to be reduced with the incorporation of the Cu in the films. The effects of Cu doping on the *c*-orientation of ZnO films have been inconsistently reported. Lee et al. reported an increase of the *c*-orientation peak by Cu doping.[11] On the contrary, Bashi et al. reported an decrease of the *c*-orientation peak by Cu doping.[20] There are numerous ideas about the reason of the effects of Cu doping on the *c*-orientation in ZnO thin films. Our Cu(7%)-doped ZnO film exhibits $Cu_2O(111)$ and (200) peak at $2\theta = 36.52$ and 42.42, respectively. The ionic radii of Cu^{2+} (0.057 nm) and Cu^{+} (0.060 nm) are same as or smaller than that of Zn^{2+} (0.060 nm). Therefore, the increase in the lattice parameters a and c cannot be solely explained by ionic radii difference.[19,20]

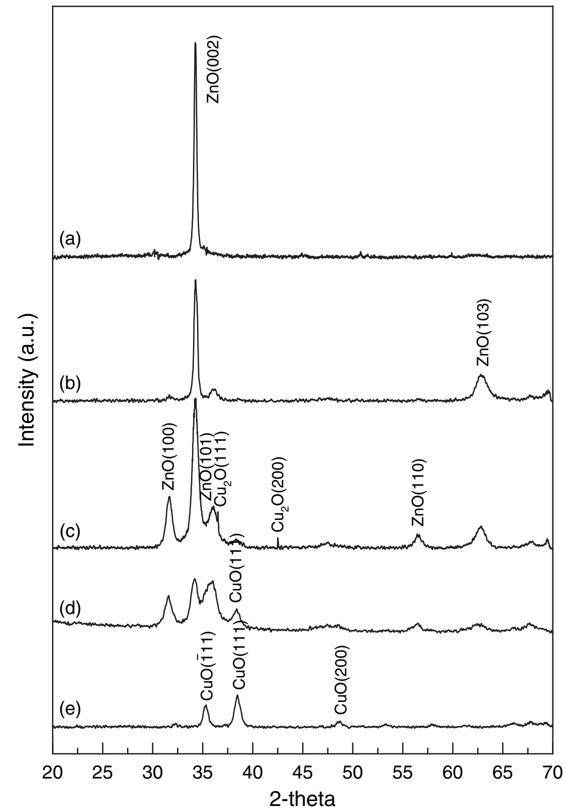

Fig. 1. XRD patterns of ZnCuO films as a function of Cu concentrations: (a) ZnO, (b) Cu(5%)-doped ZnO, (c) Cu(7%)-doped ZnO, (d) Cu(9%)-doped ZnO, and (e) CuO.

Figure 2 shows transmittance spectra measured at room temperature by a UV-VIS spectrophotometer. The average transmittance of the undoped ZnO film is above 85% in the visible wavelength region. However, the transmittances of ZnCuO films decrease with the increase of the Cu concentration, which is consistent with the results of optical transmission spectra in a reference.[21,22] The optical band

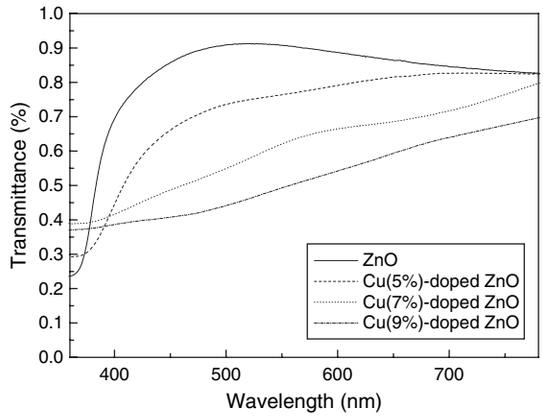

Fig. 2. Transmittance of ZnCuO films as a function of Cu concentrations.

gap of the ZnO thin films was estimated by the extrapolation of the linear portion of $(\alpha h\nu)^2$ versus $h\nu$ plots using the relation $\alpha h\nu = A(h\nu - E_g)^n$ where $h\nu$ is the photon energy, α the absorption coefficient, E_g the band gap, A the constant, and $n = 1/2$, 3/2, 2, and 3 according to the transitions of direct-allowed, direct-forbidden, indirect-allowed, and indirect-forbidden, respectively.[21, 22]

The ZnCuO film is also known to be a direct-allowed semiconductor. Therefore, the extrapolation of the straight line down to the point of $(\alpha h\nu)^2 = 0$ gives the value of the energy band gap. From the measurement of the optical transmittance and the calculated absorption coefficients, the band-gap energies of the ZnCuO films were determined, as shown in Figure 3.

The obtained energy band gaps of ZnO, Cu(5%)-doped ZnO, Cu(7%)-doped ZnO, and Cu(9%)-doped ZnO films are 3.14, 2.64, 2.05, and 1.89, respectively. While the band gap of undoped ZnO film was closed to the previously reported value, the band gaps of the ZnCuO films decreased with their Cu concentrations.[14, 20] Nakano et al. reported that the Cu_2O-based *p*-type transparent

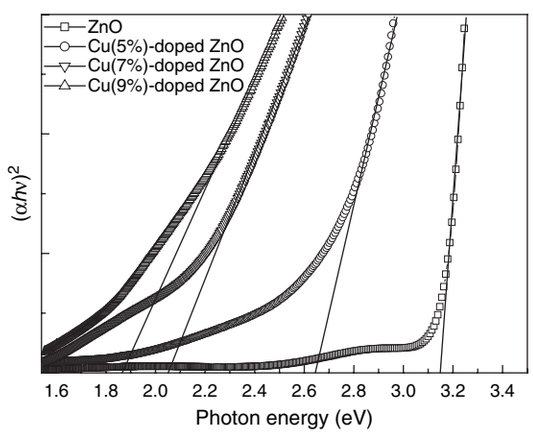

Fig. 3. Energy band gap of ZnCuO films as a function of Cu concentrations.

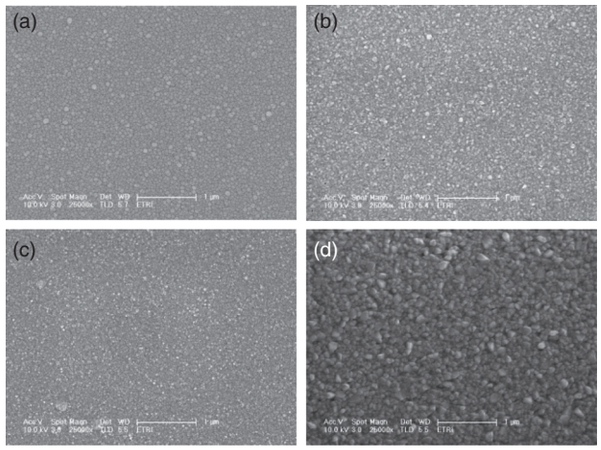

Fig. 4. SEM images of ZnCuO films as a function of Cu concentrations: (a) ZnO, (b) Cu(5%)-doped ZnO, (c) Cu(7%)-doped ZnO, and (d) Cu(9%)-doped ZnO.

conductive oxides such as $CuAlO_2$ and $SrCu_2O_2$ also have a reduced energy band-gap structure due to the reduction of the oxygen-mediated *d–d* coupling energy between Cu atoms.[23, 24] This mechanism of the band-gap reduction, however, could not be directly applied to the ZnCuO system in this study, since the ZnCuO films in this study did not have a single ZnCuO phase but multi-phases of CuO, Cu_2O, and ZnO, as can be seen in the XRD data [see Figs. 1(c and d)]. The SEM images of the ZnCuO films as functions of the Cu concentration are shown in Figure 4. It can be seen from the figures that the films had various surface morphologies. Interestingly, the average grain size increased abruptly when the Cu concentration increased from 7% to 9% [see Figs. 4(c and d)], which may be related to the CuO-phase polycrystalline, as expected from the XRD pattern [see Fig. 1(d)].

The electrical properties were estimated using a Hall measurement in the van der Pauw configuration. The type of conductivity was confirmed from the sign of Hall coefficient. The electrical properties are summarized in Table I.

The as-deposited films showed *n*-type conductivity. When annealed, the conductivity changed to the *p* type for the 7% Cu-doped films, where the Cu_2O phase existed [see Fig. 1(c)]. The type of conductivity reveals that the films become *p*-type conducting when they crystallize in the

Table I. Electrical properties of ZnCuO films as a function of Cu concentration with heat treatment.

Cu concentration	Resistivity (Ω-cm)	Hall mobility (cm^2/Vs)	Carrier concentration (cm^{-3})	Conduction type
ZnO	100	20	6×10^{15}	*n*
Cu 5% doped ZnO	22.24	0.19	1.47×10^{18}	*n*/*p*
Cu 7% doped ZnO	17.28	0.27	1.33×10^{19}	*p*
Cu 9% doped ZnO	2.85	0.13	1.31×10^{18}	*n*/*p*
CuO	—	—	—	—

RESEARCH ARTICLE

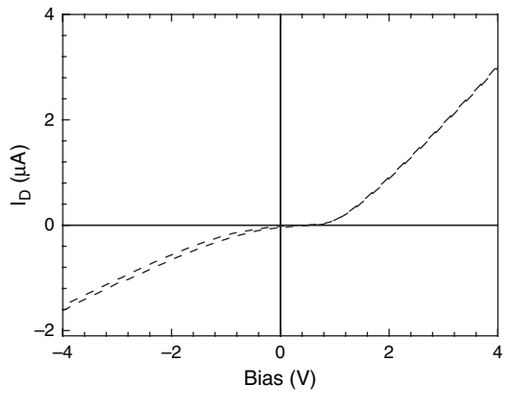

Fig. 5. Room temperature I–V characteristic of ZnCuO/IZO p–n junction.

Cu_2O phase. In general, most oxides exhibit poor mobility of holes in the valence band because the O 2p states of the upper valence band are localized. Exceptionally, in Cu_2O, the top of the valence states is derived from fully occupied Cu 3d states that are close to the O 2p states and are more mobile when converted into holes.[5, 11]

Figure 5 shows a typical current–voltage (I–V) characteristic of the grown p-ZnCuO/n-IZO hetero-junction structure by sputtering. A rectifying effect of this p–n junction was observed. The current–voltage curves of this p–n junction diode were affected by electrical properties of the p-type ZnCuO layer. The characteristics showed the rectifying nature of this p–n junction with a typical forward to reverse current ratio of ∼2.1 in the bias range of −4 to +4 V. The turn-on voltage of the p–n junction is found to have been ∼0.7 V. The turn-on voltage, which was also identified as the diffusion or built-in potential, might be a potential barrier such that the carriers have to overcome it to contribute to forward current.[25, 26] The Cu(5%) and Cu(9%)-doped ZnO films did not show this phenomenon, though. The n-type IZO layer deposited by rf sputtering was amorphous, and the co-sputtered ZnCuO layer was poly-crystalline, which could lead to structural imperfections at grain boundaries and at the interface, which, in turn, could lead to the deterioration of the diode quality.[25]

Figure 6 shows the I_{ds}–V_{gs} measurement results of the fabricated bottom-gate ZnCuO TFTs with the 7% Cu-doped ZnO film as an active channel layer. The I_{ds}–V_{gs} measurements were performed in both the linear region ($V_{DS} = -1$ V) and the saturation region ($V_{DS} = -20$ V), as shown in Figure 6. The transfer characteristics (I_{ds}–V_{gs}) of the ZnCuO TFTs exhibited a p-type nature. Thus, the drain current (I_{ds}, the y-axis on the left of Fig. 6) increased with the negative gate voltage. The on-off drain current ratio ($I_{on/off}$) was ∼6, and the field effect mobility was ∼0.01 cm^2/Vs. These results show that further experiments are required to improve the electrical characteristics of ZnCuO TFTs.

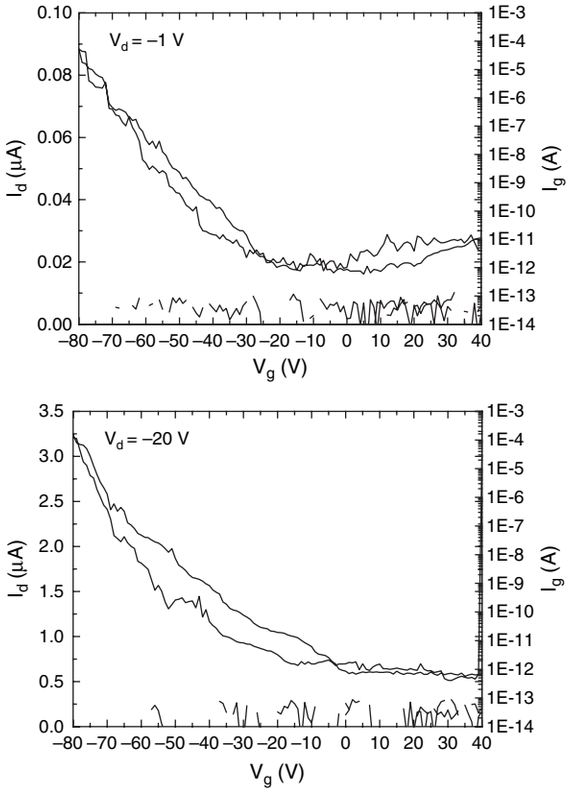

Fig. 6. Transfer characteristics of p-type ZnCuO TFT (a) $V_{DS} = -1$ V and (b) $V_{DS} = -20$ V.

4. CONCLUSIONS

Polycrystalline p-type semiconducting ZnCuO thin films were obtained by co (dc and rf) magnetron sputtering. The effects of Cu concentration on the structural, optical, and electrical properties of ZnCuO films were investigated. The films were transparent in the visible region. It was observed that the band-gap energies and conduction types of the films were affected by Cu_2O phase. The p-type conductivity was confirmed from Hall effects, p–n junctions, and bottom-gated TFTs. The TFTs with the ZnCuO channel exhibited p-channel TFT operations. The on-off drain current ratio ($I_{on/off}$) is ∼6. The results of this study indicate the possibility of the application of the ZnCuO thin films with variable band-gap energies to ZnO-based optoelectronic devices.

Acknowledgments: This work was supported by the IT R&D program of MKE/KEIT [2006-S079-05. Smart window with transparent electronic devices].

References and Notes

1. Q. Gu, T. Tanaka, M. Nishio, and H. Ogawa, *J. J. Appl. Phys*. 45 (**2007**).
2. J-.H. Shin, J-.S. Lee, C-.S. Hwang, S-.H. Ko Park, W-.S. Cheong, M. K. Ryu, C-.W. Byun, J-.I. Lee, and H. Y. Chu, *ETRI J.* 31 (**2009**).

3. W-.S. Cheong, J-.M. Lee, J-.H. Lee, S-.H. Ko Park, S. M. Yoon, C-.W. Byun, S. H. Yang, S. M. Chung, K. I. Cho, and C-.S. Hwang, *ETRI J.* 31 **(2009)**.
4. C. Y. Zhang, *Mat. Sci. Semi. Proc.* 10 **(2007)**.
5. H. Kawazoe, M. Tasukawa, H. Hyodo, M. Kurita, H. Yangai, and H. Hosono, *Nature* 389, 939 **(1997)**.
6. T. Maemoto, N. Ichiba, S. Sasa, and M. Inoue, *Thin Solid Films* 486 **(2005)**.
7. Y. Nakano, T. Morikawa, T. Ohwaki, and Y. Taga, *Appl. Phys. Lett.* 88, 172103 **(2006)**.
8. H. S. Yang, Y. Li, D. P. Norton, K. Ip, and S. J. Pearton, *Appl. Phys. Lett.* 86, 192103 **(2005)**.
9. X. Pan, Z. Ye, J. Li, X. Gu, Y. Zeng, H. He, L. Zhu, and Y. Che, *Appl. Sur. Sci.* 253 **(2007)**.
10. A. N. Banerjee, S. Kundoo, and K. K. Chattopadhyay, *Thin Solid Films* 440 **(2003)**.
11. J-.B. Lee, H-.J. Lee, S-.H. Seo, and J-.S. Park, *Thin Solid Films* 398 **(2001)**.
12. E. M. Alkoy and P. J. Kelly, *Vac.* 79 **(2005)**.
13. T. S. Herng, S. P. Lau, S. F. Yu, H. Y. Yang, X. H. Ji, J. S. Chen, N. Yasui, and H. Inaba, *J. Appl. Phys.* 99 **(2006)**.
14. H-.J. Lee, B-.S. Kim, C. R. Cho, and S-.Y. Jeong, *Phy. Stat. Sol (b)* 241 **(2004)**.
15. D. B. Buchholz, R. P. H. Chang, J. H. Song, and J. B. Ketterson, *Appl. Phys. Lett.* 87, 082504 **(2006)**.
16. J. Huso, J. L. Morrison, J. Mitchell, E. Casey, H. Hoeck, C. Walker, L. Bergman, W. M. H. Oo, and M. D. McCluskey, *Appl. Phys. Lett.* 94, 061919 **(2009)**.
17. X. Peng, J. Xu, H. Zang, B. Wang, and Z. Wang, *J. Lumin.* 128 **(2008)**.
18. M. Ötas and M. Bedir, *Thin Solid Films* 516 **(2008)**.
19. D. Bao, H. Gu, and A. Kuang, *Thin Solid Films* 312 **(1998)**.
20. Z. B. Bahşi and A. Y. Oral, *Optical Materials* 29 **(2007)**.
21. K. Samata, P. Bhattacharya, and R. S. Katiyar, *J. Appl. Phys.* 105 **(2009)**.
22. V. Figueiredo, E. Elangovan, G. Gonçalves, P. Barquinha, L. Pereira, N. Franco, E. Alves, R. Martins, and E. Fortonato, *Appl. Surf. Sci.* 254 **(2008)**.
23. Y. Nakano, S. Saeki, and T. Morikawa, *Appl. Phys. Lett.* 94, 022111 **(2009)**.
24. A. Kudo, H. Yanagi, H. Hosono, and H. Kawazoe, *Appl. Phys. Lett.* 73, 220 **(2009)**.
25. R. S. Ajimsha, K. A. Vanaja, M. K. Jayaraj, P. Misra, V. K. Dixit, L. M. Kukerja, *Thin Solid Films* 515 **(2007)**.
26. K. Matsuzaki, K. Nomura, H. Yanagi, T. Kamiya, M. Hirano, and H. Hosono, *Appl. Phys. Lett.* 93, 202107 **(2008)**.

Received: 31 July 2009. Accepted: 27 November 2009.